Journal of Hazardous Materials 357 (2018) 424–430

Contents lists available at ScienceDirect

Journal of Hazardous Materials

journal homepage: www.elsevier.com/locate/jhazmat

Heavy-ion irradiation effects on U_3O_8 incorporated $Gd_2Zr_2O_7$ waste forms

Xirui Lu[a,*], Xiaoyan Shu[a], Shunzhang Chen[a], Kuibao Zhang[a], Fangtin Chi[a], Haibin Zhang[b,*], Dadong Shao[c], Xueli Mao[a]

[a] *Fundamental Science on Nuclear Wastes and Environmental Safety Laboratory, Southwest University of Science and Technology, Mianyang, Sichuan, 621010, PR China*
[b] *Institute of Nuclear Physics and Chemistry, China Academy of Engineering Physics, Mianyang, Sichuan 621010, PR China*
[c] *Institute of Plasma Physics, Chinese Academy of Sciences, P.O. Box 1126, Hefei, 230031, PR China*

ARTICLE INFO

Keywords:
$Gd_2Zr_2O_7$pyrochlore
U_3O_8
Heavy-ion irradiation
Radiation tolerance
Amorphization

ABSTRACT

In this research, the heavy-ion irradiation effects of U-bearing $Gd_2Zr_2O_7$ ceramics were explored for nuclear waste immobilization. U_3O_8 was designed to be incorporated into $Gd_2Zr_2O_7$ from two different routes in the form of $(Gd_{1-4x}U_{2x})_2(Zr_{1-x}U_x)_2O_7$ ($x = 0.1, 0.14$). The self-irradiation of actinide nuclides was simulated by Xe^{20+} heavy-ion radiation under different fluences. Grazing incidence X-ray diffraction (GIXRD) analysis reveals the relationship between radiation dose, damage and depth. The radiation tolerance is promoted with the increment of U_3O_8 content in the discussed range. Raman spectroscopy testifies the enhancement of radiation tolerance and microscopically existed phase evolution from the chemical bond vibrations. In addition, the microstructure and elemental distribution of the irradiated samples were analyzed as well. The amorphization degree of the sample surface declines as the U content was elevated from $x = 0.1$ to $x = 0.14$.

1. Introduction

Since Ewing and Weber had proposed that pyrochlore was promising waste matrix of radioactive nuclides, substantial studies about the feasibility and properties of pyrochlore as waste immobilization medium have been conducted in the past decades [1–3]. The synthesis route, phase evolution, radiation damage and aqueous durability of pyrochlore-based waste materials have been comprehensively studied [4–7]. In the pyrochlore family, $Gd_2Zr_2O_7$ was widely explored for nuclear waste immobilization because of its excellent stability over geological time scale [7–10]. Due to its flexible crystal structure with typical $A_2B_2O_7$ stoichiometry, $Gd_2Zr_2O_7$ holds the capacity to accommodate actinides and lanthanides into the eight-coordinate A-site with Zr occupy the six-coordinate B-site [8]. Meanwhile, there are two different oxygen sites in the pyrochlore structure. Six O(1) atoms occupy the 48*f* sites, which are surrounded by two A^{3+} cations and two B^{4+} cations. One O(2) atom occupies the 8*b* site and is in tetrahedral coordination with only A^{3+} cations. The remaining unoccupied interstitial site at 8*a* is surrounded by B^{4+} cations [8,11]. The crystal structure of pyrochlore is very sensitive to the incorporated substitution elements, which induces phase transformation between pyrochlore and defect fluorite. The stability of pyrochlore structure is governed by the radius ratio of cation A^{3+} and B^{4+} (r_A/r_B) [11,12].

For nuclear waste immobilization, U_3O_8 was widely used as the surrogate material because of its concurrently existed valence state of U^{4+} and U^{6+} [13–16]. In our previous study, U_3O_8 was designed to be incorporated into $Gd_2Zr_2O_7$ pyrocholre from two different routes to improve the solid solubility, where U^{4+} occupied Zr^{4+} site for equivalent substitution while U^{6+} replaced Gd^{3+} site for unequivalent substitution [17]. The solubility of U_3O_8 in $Gd_2Zr_2O_7$ and its impact on the phase composition and microstructure have been discussed. This type of ceramic waste form contains a defective fluorite phase within the solid solubility range. And the loading capacity of U_3O_8 can be promoted up to 38.83 *wt.*% in this $Gd_2Zr_2O_7$ waste form.

Radiation stability is an important consideration for nuclear waste form as it will be buried in deep geological repository. The resistance of phase evolution or radiation induced amorphization were typically analyzed to evaluate the long-term radiation stability. J. Shamblin et al. indicate that r_A/r_B is clearly a dominating factor in predicting track size and damage morphology, which could even be extended to other compositionally related complex oxides [18]. Moreover, C. Chung et al. disclose that the damage recovery of $Dy_2Ti_2O_7$ involves multistep processes with decoupled long-range recrystallization and short-range defect recovery. The damaged sample is not fully recovered, structurally or energetically, even after heating well above the initial recrystallization temperature [19]. In our previous work, the effects of alpha particle irradiation have been studied as well using the $(Gd_{1-4x}U_{2x})_2(Zr_{1-x}U_x)_2O_7$ ($x = 0.1, 0.14$) system [20]. The results reveal that the higher U doping amount is beneficial for the improvement of radiation tolerance.

---

* Corresponding authors.
E-mail addresses: luxiruimvp116@163.com (X. Lu), wsschbinzhang@163.com (H. Zhang).

https://doi.org/10.1016/j.jhazmat.2018.06.026
Received 25 September 2017; Received in revised form 9 May 2018; Accepted 11 June 2018

Table 1

Contents of raw powders $(Gd_{1-4x}U_{2x})_2(Zr_{1-x}U_x)_2O_7$ for irradiation experiment.

x value for B-site U atoms	weights of raw powders (g)		
	Gd_2O_3	ZrO_2	U_3O_8
0.1	0.3580	0.3650	0.2771
0.14	0.2627	0.3490	0.3883

In this study, heavy-ion irradiation experiment was conducted to further investigate the radiation effects on $(Gd_{1\text{-}4x}U_{2x})_2(Zr_{1\text{-}x}U_x)_2O_7$ (x = 0.1, 0.14) pyrochlore waste forms. X-ray diffraction (XRD) and Grazing incidence X-ray diffraction (GIXRD) was employed to characterize the structure and phase evolution as a function of uranium content and involved irradiation intensity. The Raman spectra were collected to obtain the detailed local information of irradiated samples. At last, the heavy-ion irradiation induced microstructure evolution and elemental distribution were investigated as well.

2. Experimental details

2.1. Preparation of the original samples

In this study, polycrystalline $(Gd_{1\text{-}4x}U_{2x})_2(Zr_{1\text{-}x}U_x)_2O_7$ (x = 0.10, 0.14) ceramic samples were prepared from a standard solid state reaction process. The point x = 0.14 was the solubility limit in the system as a single phase based on our previous results [20], moreover, x = 0.10 was chosen to study the influence of uranium content on the irradiation effects. A.R. grade Gd_2O_3, ZrO_2 and U_3O_8 powders were purchased as the raw materials. Before weighing and mixing, all the powders were pre-heated at 70 ℃ for 12 h to remove the possibly existed moisture and other impurities. The dried powders were subsequently weighed according to Table 1 and uniformly mixed in pure ethanol. The homogenized powders were subsequently dried and moulded into a pellet form (12 mm diameter and ~2 mm thickness) at a pressure of 10 MPa. The pellets were finally sintered at 1500 ℃ for 48 h in flowing air atmosphere to fabricate compact ceramic samples.

2.2. Irradiation experiment

The heavy-ion irradiation experiments were performed at room temperature using a 320 kV multi-discipline research platform for highly charged ions at the Institute of Modern Physics, Chinese Academy of Sciences. As presented in Fig. 1, the tested pellets were prepared by cutting the bulky specimens into pieces with dimension of about 0.8 × 0.8 mm. The displacement damage at the fluence of 1×10^{15} ions/cm^2 was calculated to be about 14.35 dpa with the irradiation parameters listed in Table 2 [19]. The 1.5 MeV Xe^{20+} ions were implanted at fluences ranging from 1×10^{12} ions/cm^2 to 1×10^{15} ions/cm^2 with 5×10^{11} ions/cm^2/s flux oriented vertically onto the sample surface.

2.3. Characterizations

The phase structure of the pristine samples was confirmed by X-ray diffraction (X'Per PRO, Netherlands) with Cu Kα radiation (λ = 1.5406 Å), operating at 2.2 kW. The 2θ range of collected data was 10° - 90°, with a scanning rate of 2°/min. The evolution of phase composition and crystal structure after irradiation were analyzed using grazing incidence X-ray diffraction (GIXRD, X'Pert PRO, Netherlands) with Cu Kα radiation (λ = 1.5406 Å). The 2θ range of collected data is 10-80° with a scanning speed of 2°/min. The structural evolution of irradiated samples was characterized by a Raman spectrometer (Renishaw inVia, U.K.) equipped with Argon ion laser. Considering the sensitivity to different laser wavelength, the incident laser beam (785 nm) of the Raman microscope was chosen to be focused on all the samples through a 50× dry objective to the spot of about 2 μm. Power 1.7 mW was used to examine the samples, with the exposure time was 10 s, 2 scans. Field emission scanning electron microscopy (FESEM, Zeiss Ultra-55, Oberkochen, Germany) was utilized to observe the microstructure evolution of irradiated samples. The elemental distribution was analyzed using energy-dispersive X-ray spectrometer (EDX) attached to the FESEM equipment. Sub-microstructure of the irradiated samples was observed by transmission electron microscopy (TEM, Libra 200 FE, Germany). Before testing in a plane-view, the samples were prepared by mechanical thinning, dimpling and ion milling under Ar ions until perforation.

3. Results and discussion

3.1. Phase evolution analysis by XRD and GIXRD

The pristine samples were firstly tested by XRD (shown in Fig. 2). As the featured super-lattice peaks of pyrochlore at $2\theta \approx 14°$, 27° and 37° are absent, we can deduce that both U-doped samples display a defect fluorite structure. Since r_A/r_B ratio for the x = 0.1 sample is 1.41 while r_A/r_B for the x = 0.14 sample is 1.39, these two values deviate from the r_A/r_B requirement of pyrochlore structure (r_A/r_B = 1.46–1.78). Compared with the x = 0.10 sample, the XRD intensity of the x = 0.14 sample is higher. This indicates that the crystallinity was enhanced as the U incorporation was elevated from x = 0.10 to x = 0.14, which also reveals the decrement of amorphization and improvement of radiation tolerance for the x = 0.14 sample.

The irradiated $(Gd_{1\text{-}4x}U_{2x})_2(Zr_{1\text{-}x}U_x)_2O_7$ (x = 0.1, 0.4) samples were

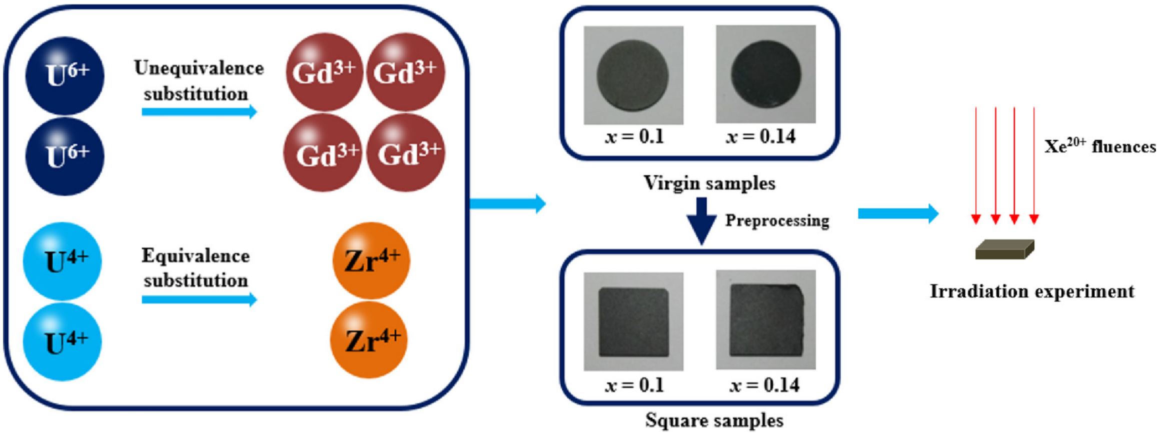

Fig. 1. The process of fabrication and irradiation experiment.